Three-Dimensional Perturbations on Hypersonic Wedge Flow

NORMAN D. MALMUTH*
North American Aviation, Inc., Los Angeles, Calif.

The hypersonic inviscid flow over a configuration representing a small perturbation about a two-dimensional wedge is analyzed. Equations and boundary conditions are obtained for a class of general perturbations within the framework of hypersonic small disturbance theory. A specialization of this formulation is made to the case where the resultant perturbation consists of two semi-infinite flat plates of slightly different incidence to the freestream. The flow over such a shape is divided into an outlying uniform region and a central conefield. The determination of the conefield gives rise to an elliptic boundary-value problem, which is solved with the aid of the Tschaplygin transformation and other conformal mappings. Calculations are presented using a Fourier series solution for the perturbation pressure which yields the surface loads associated with the perturbation as well as the shock distortion function. Integral representations are obtained for the downwash and sidewash perturbations from the pressure solution. The results are compared qualitatively with an analogous linear supersonic flow. Finally, a solution for more general profiles is obtained under the further restriction that the specific heat ratio γ is close to one. This solution is specialized to the configuration considered previously.

Nomenclature

A_n	= Fourier coefficient
B	= body function
B_n	= nA_n
C_n	= $2B_n \cosh 2n\sigma_0$
D	= convective operator of basic flow
G	= conical shock distortion function
H	= hypersonic similarity parameter
L	= elliptic operator
M	= Mach number
P	= pressure
S	= shock function
U	= freestream velocity
Z	= conical reduced variable = z/cx
c	= $[\gamma(\gamma-1)/2]^{1/2}$ = perturbation sound speed
f	= body distortion function
g	= shock distortion function
$\mathbf{i},\mathbf{j},\mathbf{k}$	= unit vectors along $\bar{x}$, $\bar{y}$, $\bar{z}$ axes, respectively
p	= normalized pressure
$\mathbf{q}$	= resultant velocity vector
u,v,w	= velocity perturbations in $\bar{x}$, $\bar{y}$, $\bar{z}$ directions, respectively (backwash, downwash, sidewash)
$\bar{x},\bar{y},\bar{z}$	= Cartesian axes
x,y,z	= distorted Cartesian axes, in HSDT (hypersonic small disturbance theory) limit
x^*,y^*,z^*	= distorted Cartesian axes in Newtonian approximation
β	= cotangent of Mach angle
γ	= specific heat ratio
δ	= dimensionless wedge thickness ratio
ϵ	= wedge perturbation parameter
ζ	= complex variable
θ	= wave angle associated with basic wedge
λ	= $(\gamma-1)/(\gamma+1)$, limiting density ratio parameter
μ	= Mach angle, ordinate
ν	= complex varable
ρ	= density
σ	= abscissa
ψ	= stream function of undisturbed flow
ω	= dummy variable
Ψ	= ψ/cx = reduced conical variable

Subscripts

0	= from basic flow
1	= behind basic shock
∞	= corresponding to freestream conditions

Received June 10, 1963; revision received March 18, 1964. The author is indebted to J. D. Cole of the California Institute of Technology for his many suggestions and criticisms.

* Research Specialist. Member AIAA.

I. Introduction

LITTLE theoretical information is available at present to guide the aeronautical engineer in the analysis and design of hypersonic control surfaces. In this connection, a fundamental problem, which occurs frequently in technical applications, is the mutual interaction of adjacent lifting panels of slightly differing incidence to the freestream. Problems of this type and a number of others, such as those associated with aeroelastic distortions and boundary-layer induced interactions with an inviscid field, may be conceived as involving small perturbations about some basic flow.

To gain qualitative insight into the nature of the nonlinear phenomena associated with such perturbations, a number of investigations have been made recently involving wedge flow as the basic field. Within the framework of hypersonic small disturbance theory as given by Van Dyke and as described in Refs. 1–3, Guiraud[4] has analyzed a class of two-dimensional wedge perturbations. Holt and Yim[5] generalize the problem by using the exact equations for two special types of three-dimensional distortions. Analysis of both investigations indicates that the essential simplification resulting from the assumption on the body shape is a linearization of the flow. This conclusion follows from the reasoning that, if δ is the wedge angle and M_∞ is the freestream Mach number, a perturbation having a characteristic height of $O(\delta\epsilon)$ as $\epsilon, \delta \to 0$ gives rise to a local supersonic field characterized by the Van Dyke hypersonic-supersonic similarity parameter, $M_1\delta\epsilon = O(\epsilon)$ and $M_1 = O(1/\delta)$, where M_1 is the Mach number behind the wedge bow shock. Consequently, a requirement of linear supersonic flow is met in some neighborhood of the perturbation. However, since the bow shock is strong, the wave system that emanates from the perturbed body produces shock distortions which induce entropy and vorticity variations in the flow and make it rotational. Because of these effects, the flow structure can be anticipated to differ significantly from the usual model given by linearized theory.

The present work will obtain more information on the nature of these vortical phenomena, specifically, as they arise in certain technically important conefields, particularly those associated with the differentially deflected panel configuration just mentioned and treated superficially in Ref. 5. A brief description will also be given of the calculation of the field associated with more general perturbations under the further restrictive assumption that γ, the specific heat ratio of the flow, is near unity.

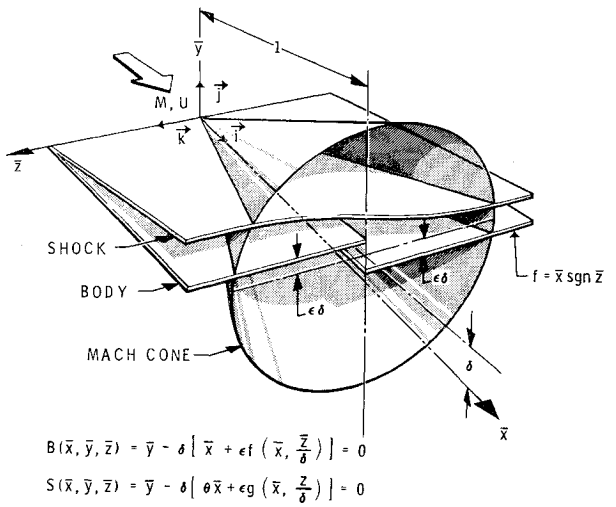

Fig. 1 Geometry of problem.

II. Basic Equations

With regard to the conefield problem mentioned in the Introduction, the differential flap configuration shown in Fig. 1 will be analyzed. According to the axis convention shown, the equation of the body surface is given by

$$B(\bar{x},\bar{y},\bar{z}) = \bar{y} - \delta\bar{x}(1 + \epsilon\,\mathrm{sgn}\bar{z}/\delta) = 0 \tag{1}$$

where

$$\mathrm{sgn}x = 1, \quad x > 0 \qquad \mathrm{sgn}x = -1, \quad x < 0$$

and that of the shock very nearly by

$$S(\bar{x},\bar{y},\bar{z}) = \bar{y} - \delta[\theta\bar{x} + \epsilon g(\bar{x},\bar{z}/\delta)] = 0 \tag{2}$$

in the limit,

$$H \equiv 1/M^2\delta^2 \to 0 \quad \text{as} \quad \delta,\epsilon \downarrow 0 \text{ independently}\dagger \tag{3}$$

For (3), the flow about the basic wedge described by the first two terms in Eq. (1) corresponds to that of Van Dyke's hypersonic small disturbance theory. The function g appearing in Eq. (2) obviously represents the perturbation of the basic planar shock of wave angle, θ arising from the wedge distortion. The role of δ, as it appears in the second argument of the shock perturbation function g, is to preserve similarity in the HSDT limit, Eq. (3). In this limit, the asymptotic representations of the velocity vector $\mathbf{q}$, pressure P, and density ρ are

$$\mathbf{q}(\bar{x},\bar{y},\bar{z};\ M,\delta,\epsilon)/U = \mathbf{i}[1 + O(\delta^2)] + \mathbf{j}\delta[v_0 + \epsilon v(x,y,z;\ H)] + \mathbf{k}\delta\epsilon w + \ldots \tag{4a}$$

$$P - P_\infty/\rho_\infty U^2 = \delta^2 p_0(1 + \epsilon p) + \ldots \tag{4b}$$

$$\rho/\rho_\infty = \sigma_0(1 + \epsilon\sigma) + \ldots \tag{4c}$$

where

$$x = \bar{x} \qquad y = \bar{y}/\delta \qquad z = \bar{z}/\delta \tag{5}$$

and the undistorted wedge quantities are denoted by subscript 0.

The exact equations for the gas motion are

Continuity

$$\nabla\cdot\rho\mathbf{q} = 0 \tag{6a}$$

Momentum

$$\mathbf{q}\cdot\nabla\mathbf{q} = -\nabla P/\rho \tag{6b}$$

Entropy

$$\mathbf{q}\cdot\nabla P/\rho^\gamma = 0 \tag{6c}$$

† The present analysis can be easily extended to the more general limit, H fixed as $\delta, \epsilon \downarrow 0$, independently. The limit, (3), was selected for convenience.

where

$$\nabla \equiv \mathbf{i}\partial/\partial\bar{x} + \mathbf{j}\partial/\partial\bar{y} + \mathbf{k}\partial/\partial\bar{z}$$

Substitution of the expansions (4) into the equations of motion (6), gives rise to the following equations for the perturbation quantities:

$$Du = -(p_0/\sigma_0)p_x \tag{7a}$$

$$Dv = -(p_0/\sigma_0)p_y \tag{7b}$$

$$Dw = -(p_0/\sigma_0)p_z \tag{7c}$$

$$D(p - \gamma\sigma) = 0 \tag{7d}$$

$$\sigma_x + v_y + v_0\sigma_y + w_z = 0 \tag{7e}$$

where

$$D \equiv \partial/\partial x + v_0\partial/\partial y \tag{7f}$$

By application of the hypersonic limit, (3) to two-dimensional wedge flow, the following results for the zero-order quantities are obtained:

$$v_0 = 1 \tag{8a}$$

$$p_0 = (\gamma + 1)/2 \tag{8b}$$

$$\sigma_0 = (\gamma + 1)/(\gamma - 1) \tag{8c}$$

$$\theta = (\gamma + 1)/2 \tag{8d}$$

Substitution of Eqs. (2, 4, and 8) into the basic conservation laws that hold at the shock gives the following relations:

$$p_S \doteq p(x,(\gamma + 1)/2,z) = 2v_S \tag{9a}$$

$$v_S = 2g_x/(\gamma + 1) \tag{9b}$$

$$w_S = -g_z \tag{9c}$$

Here, one of the dominantly simplifying features of the assumption of small perturbations becomes apparent. Since the distorted shock is close to its undistorted counterpart, it is possible to linearize and satisfy the boundary conditions on the undisturbed surface.

The typical inviscid boundary condition at the body similarly applied yields

$$v_B \doteq v(x,0,z) = \mathrm{sgn}z \tag{10}$$

For the more general case where

$$B = \bar{y} - \delta[\bar{x} + \epsilon f(\bar{x},\bar{z}/\delta)] = 0 \tag{11}$$

Eq. (10) changes to

$$v_B = f_x \tag{12}$$

In all other respects, the flow model remains unchanged, i.e., Eqs. (7, 8, and 9) are unaltered for the configuration described by (11). Since no major conceptual differences in basic flow structure are anticipated in going from configuration (1) to (11), the discussion for $\gamma \neq 1$ will be hereinafter limited to a consideration of (1) only.

III. Solution for Perturbations

Rewriting Eqs. (7), using the zeroth-order solution, (8), and Von Mises variables, where $\psi_y = 1$ and $\psi_x = -1$, ψ being the stream function corresponding to the basic wedge flow, gives

$$p_x/\gamma + v_\psi + w_z = 0 \tag{13a}$$

$$v_x + (\gamma - 1)p_\psi/2 = 0 \tag{13b}$$

$$w_x + (\gamma - 1)p_z/2 = 0 \tag{13c}$$

$$v_B = v(x,0.z) = \mathrm{sgn}z \tag{14a}$$

$$p_S = 2v_S = p[x,(\gamma - 1)x/2,z] = 4g_x/(\gamma + 1) \tag{14b}$$

$$w_S = -g_z \tag{14c}$$

The backwash, u, can be ignored at this point as being uncoupled from the problem described by Eqs. (13) and (14). This quantity can be determined later from an integration of Eq. (7a) or conservation of stagnation enthalpy. The density perturbation, σ, has also been eliminated by a substitution of (7d) into (7a).

Cross differentiation, and some manipulation between Eqs. (13), yields the following wave equation for p:

$$2p_{xx}/\gamma(\gamma - 1) - p_{\psi\psi} - p_{zz} = 0 \tag{15}$$

This, incidentally, is identical to the equation for pressure obtained by ordinary linearized supersonic wing theory and bears out the heuristic considerations of the Introduction.

In (15), the quantity $c = [\gamma(\gamma - 1)/2]^{1/2}$ can be shown to be the speed at which perturbation pressure waves travel in (ψ,z) planes. In this model, this quantity, like all other convective characteristics, is determined from the basic flow. From the Introduction, it is seen that

$$\gamma(\gamma - 1)/2 = 1/M_1^2\delta^2 = H_1 = c^2 \tag{16}$$

Determination of the Pressure

Since there is no characteristic length in the problem, the formulation given in Eqs. (13) and (14) exhibits conical similarity; hence, p, v, and w are functions of Ψ and Z only, where

$$\Psi \equiv \psi/cx \qquad Z \equiv z/cx \tag{17}$$

In addition, the shock is a ruled surface, i e.,

$$g = xG(Z) \tag{18}$$

With the assumption of conical similarity, the problem described by (13) and (14) takes on the following appearance:

$$1/B(\Psi p_\Psi + Zp_Z) - v_\Psi - w_Z = 0 \tag{19a}$$

$$p_\Psi/B - \Psi v_\Psi - Zv_Z = 0 \tag{19b}$$

$$p_Z/B - \Psi w_\Psi - Zw_Z = 0 \tag{19c}$$

$$p_S = 2v_S = p(1/B,Z) = 4(G - ZG')/(\gamma + 1) \tag{20a}$$

$$w_S = -G'/c \tag{20b}$$

$$v_B = v(0,Z) = \text{sgn}Z \tag{20c}$$

$$B \equiv [2\gamma/(\gamma - 1)]^{1/2} \tag{21}$$

Also, the wave equation transforms into

$$L[p] \equiv \{(\Psi^2 - 1)\partial^2/\partial\Psi^2 + 2\Psi Z\partial^2/\partial\Psi\partial Z + (Z^2 - 1)\partial^2/\partial Z^2 + 2\Psi\partial/\partial\Psi + 2Z\partial/\partial Z\}\, p = 0 \tag{22}$$

Equation (22) changes type across the unit circle, $\Psi^2 + Z^2 = 1$, being elliptic in the region $\Psi^2 + Z^2 < 1$ and hyperbolic for $\Psi^2 + Z^2 > 1$. The constant state solution

$$v = p/2 = \text{sgn}z \tag{23a}$$

$$w = 0 \tag{23b}$$

$$\varrho = (\gamma + 1)x\ \text{sgn}z/2 \tag{23c}$$

is found to solve the hyperbolic domain.

In order to properly pose a mixed type Poincare boundary-value problem for the elliptic region, i.e., inside $MPQTM$ in Fig. 2, the values of p_Ψ must be obtained on the linearized shock, PQ, and on the linearized body, MT, in the figure. Under suitable assumptions on the behavior of v, Eqs. (19a) and (20a) give

$$p_\Psi|_{\Psi=0} = 0 \tag{24}$$

For the value of p_Ψ at the shock, an application of the boundary conditions to Eqs. (19) yields the following system for $p_\Psi|_{\Psi=\Psi_S} \equiv p_\Psi|_S$ and $v_\Psi|_S$:

$$-(\gamma - 1)p_\Psi|_S/2\gamma + v_\Psi|_S = [1 - 4Z^2/\gamma(\gamma + 1)c^2]cG'' \tag{25a}$$

$$p_\Psi|_S - v_\Psi|_S = 4Z^2G''/(\gamma - 1)(\gamma + 1) \tag{25b}$$

The solution of (25) gives

$$p_\Psi|_S = [8\gamma/\gamma - 1]^{1/2}[1 - 2(2\gamma - 1)Z^2/(\gamma + 1)]G''/(\gamma + 1) \tag{26}$$

Hence,

$$[4Zp_\Psi/(\gamma + 1) + (a + bZ^2)p_Z]_S = 0 \tag{27}$$

where

$$a = [8\gamma/(\gamma - 1)]^{1/2}/(\gamma + 1) \tag{28a}$$

$$b = -4(2\gamma - 1)[2\gamma/(\gamma - 1)]^{1/2}/(\gamma + 1)^2 \tag{28b}$$

A symmetrical formulation is obtained if p is considered even in Ψ. Then, condition (24) is automatically satisfied. Accordingly, the final form of the boundary-value problem is as indicated in Fig. 2.

By use of the Tschaplygin transformation discussed in Refs. 7 and 8, in combination with a bilinear-logarithmic mapping, the operator L given in Eq. (22) is reduced to the Laplacian Δ, and the segment-shaped elliptic domain $SPQRS$ in Fig. 2 is simplified to one which has rectangular boundaries. This composite mapping can be shown to have the form

$$\Psi = \tanh\sigma \tag{29a}$$

$$Z = \sin\mu\ \text{sech}\sigma \tag{29b}$$

Accordingly, the boundary-value problem on p shown in Fig. 2 takes on the appearance shown in Fig. 3 under the transformation, Eqs. (29). The shaded regions are correspondences of each other under (29), and the oblique derivative condition on p at the shock, Eq. (27), has been transformed into

$$\{p_\sigma - [\gamma/2(\gamma - 1)]^{1/2}\ (\text{ctn}\mu)p_\mu\}_S = 0 \tag{30}$$

If it is assumed as a working hypothesis that the solution for p is regular and unique to the boundary-value problem associated with the region $SPQRS$, the following solution can be tailored to the boundary conditions:

$$p = \frac{4\mu}{\pi} - \sum_{n=1}^{\infty} A_n \cosh 2n\sigma \sin 2n\mu \tag{31}$$

Substitution of Eq. (31) into (30), with some trigonometric

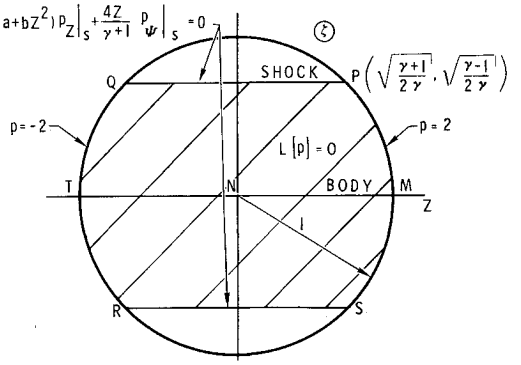

$$L[p] \equiv |(\Psi^2-1)\partial^2/\partial\Psi^2 + 2\Psi Z\partial^2/\partial\Psi\partial Z + (Z^2-1)\partial^2/\partial Z^2 + 2\Psi\partial/\partial\Psi + 2Z\partial/\partial Z|p = 0$$

$$a \equiv [8\gamma/(\gamma-1)]^{1/2}/(\gamma+1)$$

$$b \equiv -4(2\gamma-1)[2\gamma/(\gamma-1)]^{1/2}/(\gamma+1)^2$$

Fig. 2 Boundary-value problem for p in elliptic region.

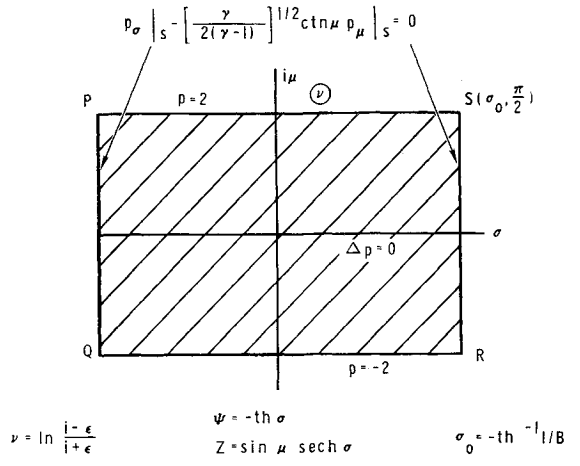

Fig. 3 Equivalent potential problem.

manipulation, yields the following two term recursion relation for the A_n:

$$-B_n/B_{n-1} = \frac{(B/2)\cosh 2(n-1)\sigma_0 + \sinh 2(n-1)\sigma_0}{(B/2)\cosh 2n\sigma_0 - \sinh 2n\sigma_0} \tag{32}$$

where

$$B_n \equiv nA_n \tag{33}$$

$$B_1 = \frac{2B/\pi}{(B/2)\cosh 2\sigma_0 - \sinh 2\sigma_0} \tag{34}$$

$$\sigma_0 \equiv -\tanh^{-1} 1/B \tag{35}$$

The solution of (32) is obviously

$$\frac{B_n}{B_{n-1}} = \prod_{k=2}^{n} \frac{B_k}{B_{k-1}}$$

From a study of the asymptotic properties of the coefficients B_n, the convergence of the series solution (31) can be deduced; i.e., it can be shown, as $n \to \infty$, that

$$-B_n/B_{n-1} \doteq [(B/2-1)/(B/2+1)]e^{-2|\sigma_0|}$$

For the series

$$S = \sum_{k=1}^{n} C_k$$

where

$$C_n = 2B_n \cosh 2n\sigma_0 \doteq B_n e^{2n|\sigma_0|} \quad \text{as} \quad n \to \infty$$

then

$$\left|\frac{C_n}{C_{n-1}}\right| = \left|\frac{1-B/2}{1+B/2}\right| \exp 2(|\sigma_0| - |\sigma_0|) \equiv r = \left|\frac{1-B/2}{1+B/2}\right|$$

That is, S is asymptotically a geometric series having its common ratio $= r$. A necessary condition for absolute convergence of the series is that

$$\lim_{n\to\infty} |C_n/C_{n-1}| = r < 1$$

that is,

$$|B/2 - 1| < |B/2 + 1|$$

which is seen to hold in this case for all γ. Hence, the S series is absolutely convergent so that the series in (31) has the same property by the comparison test. Thus, the previous assumption of the regularity of p is verified.

Figures 4a and 4b show the results of calculations made of the surface pressure distribution using the IBM 7090 computer. In addition, the first 10 An's are listed in Table 1.

Calculation of the Shock Distortion Function G

By substitution of the solution for p in the boundary condition, Eq. (20a), a first-order ordinary differential equation for G, is obtained. The solution of this equation is

$$\frac{G}{Z} - [\gamma(\gamma+1)]^{1/2} = -\frac{\gamma+1}{4} \int_{-[(\gamma+1)/2\gamma]^{1/2}}^{Z} \frac{p_S(\omega)d\omega}{\omega^2}$$

where

$$p_S(Z) \equiv p(Z, 1/B)$$

Results of numerical calculations for G are shown in Fig. 4c for $\gamma = \frac{7}{5}$. The figure shows that the shock is fairly planar over most of the interaction region, with a large curvature at the region's extremities in order to achieve transition with the outlying plane sections. A subsequent discussion of an

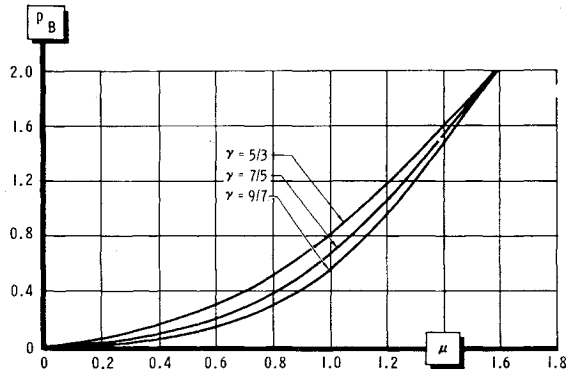

Fig. 4a Effect of specific heat ratio on surface pressures.

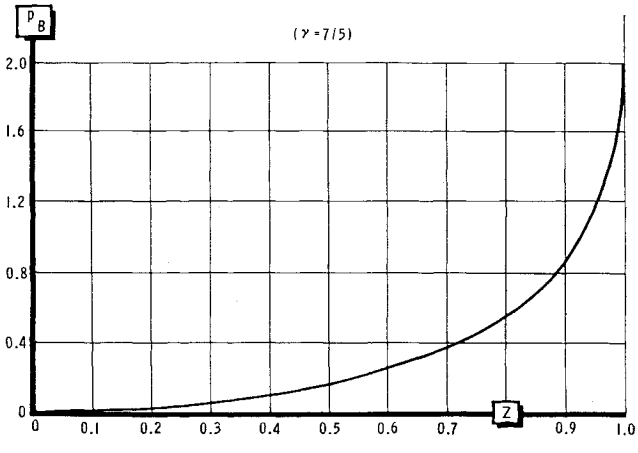

Fig. 4b Surface pressure distribution as a function of Z.

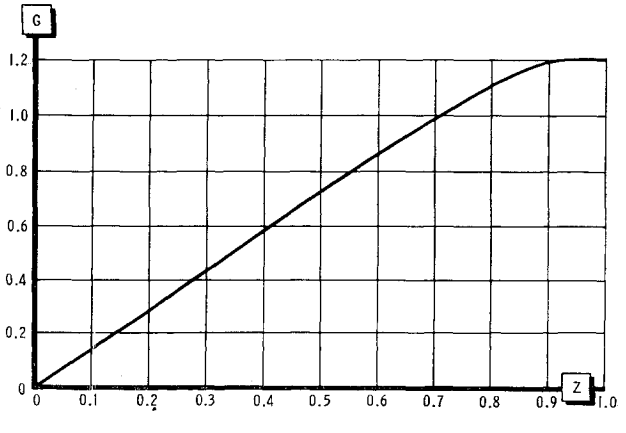

Fig. 4c Shock distortion function for $\gamma = \frac{7}{5}$.

analysis of the profile given by Eq. (1) for the limit $\gamma \to 1$ will show that this transition region shrinks to a point, i.e., the shock surface consists of three planes, and the sidewash will exhibit discontinuities along the lines of intersection of these planes.

Evaluation of the Velocities

To obtain the remaining portion of the solution involving the velocities v and w, the conical system, Eq. (19), is rewritten, using the polar coordinates

$$\Psi = R\sin\theta \tag{36a}$$

$$Z = R\cos\theta \tag{36b}$$

as independent variables. Accordingly,

$$\frac{R}{B}\frac{\partial p}{\partial R} - \left(\sin\theta\frac{\partial}{\partial R} + \frac{\cos\theta}{R}\frac{\partial}{\partial\theta}\right)v - \left(\cos\theta\frac{\partial}{\partial R} - \frac{\sin\theta}{R}\frac{\partial}{\partial\theta}\right)w = 0 \tag{37a}$$

$$R\frac{\partial v}{\partial R} = \frac{1}{B}\left(\sin\theta\frac{\partial}{\partial R} + \frac{\cos\theta}{R}\frac{\partial}{\partial\theta}\right)p = \frac{p_\Psi}{B} \tag{37b}$$

$$R\frac{\partial w}{\partial R} = \frac{1}{B}\left(\cos\theta\frac{\partial}{\partial R} - \frac{\sin\theta}{R}\frac{\partial}{\partial\theta}\right)p = \frac{p_Z}{B} \tag{37c}$$

By integration along a ray $\theta = \text{const}$ from the point (R,θ) to the boundary point $[R_B(\theta),\theta]$, it is possible to obtain from Eqs. (37b) and (37c) the solutions

$$v(R,\theta) = v(R_B,\theta) + \int_R^{R_B}\frac{p_\Psi(\rho,\theta)}{B\rho}\,d\rho \tag{38a}$$

$$w(R,\theta) = w(R_B,\theta) + \int_R^{R_B}\frac{p_Z(\rho,\theta)}{B\rho}\,d\rho \tag{38b}$$

If the quantities

$$\tan\theta_0 = [(\gamma-1)/(\gamma+1)]^{1/2} \qquad (0 < \theta_0 < \pi/2)$$

$$v_B = v(R_B,\theta) \qquad w_B = w(R_B,\theta)$$

are defined, then Table 2 gives the appropriate values of R_B and v_B, u_B corresponding to the indicated ranges of θ (cf. Fig. 5).

The forementioned values, when substituted into Eqs. (38a) and (38b), give solutions corresponding to the indicated regions. The complexity of the integrands has thus far prevented further reduction of these formulas.

From a study of the solution for p as $R \to 0$, it may be concluded that v and w exhibit the following singular behavior in the vicinity of the origin:

$$v \doteq fn(\theta) \qquad \text{as } R\to 0 \tag{39a}$$

$$w \doteq \ln R \tag{39b}$$

Table 1 Fourier coefficients for pressure

A_1	=	0.63661978
A_2	=	$-0.48970751 \times 10^{-1}$
A_3	=	$0.26573275 \times 10^{-2}$
A_4	=	$-0.13263367 \times 10^{-3}$
A_5	=	$0.67400558 \times 10^{-5}$
A_6	=	$-0.35331404 \times 10^{-6}$
A_7	=	$0.19011805 \times 10^{-7}$
A_8	=	$-0.10439105 \times 10^{-8}$
A_9	=	$0.58224602 \times 10^{-10}$
A_{10}	=	$-0.32880426 \times 10^{-11}$

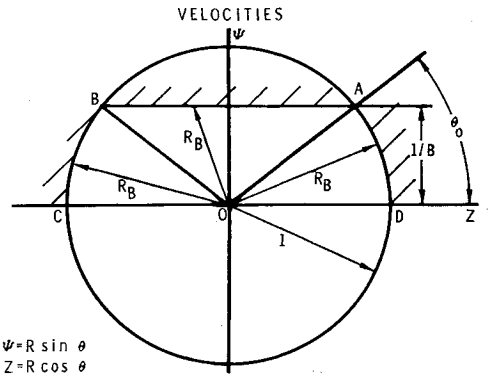

Fig. 5 Regions for velocity calculation.

IV. Comparison with Linear Supersonic Flow

If an analogous configuration in linear supersonic flow is considered relative to the hypersonic field previously discussed, it is seen that the governing equations are similar, the basic assumption that the streamlines are very nearly parallel to the x axis holds, and the similarity parameter in both flow regimes is small.

The significant differences between the two cases result from three conditions. First, in the linear supersonic flow the velocity perturbation in the freestream direction is of the same order as those in the cross-flow direction, whereas in the hypersonic regime it is of a higher order. Second, the vortical effects arising from the perturbation of the supersonic shock are only of the order of δ^3 and can be ignored, whereas the hypersonic shock is so strong that these effects must be taken into consideration. Mathematically, this means that the linear problem involves piecewise constant boundary conditions, whereas, in the hypersonic case, the dependent variables are functions of an unknown shock distortion function along the boundaries which has to be determined as part of the solution. Finally, because the vorticity in the linear case is of $O(\delta^3)$, the velocity vector is solenoidal in the first approximation, and a velocity potential function can be introduced as a dependent variable, a simplification that is not possible in the hypersonic case.

By applying the procedures given in Ref. 8, it is possible to obtain a solution to the linear problem using function-theoretic methods. From this solution, it is seen that the velocities exhibit a singular character similar to that shown in the previous hypersonic flow problem. However, the hypersonic pressure distribution, when suitable normalizations and adjustments of levels are applied, undercuts its linearized counterpart.

V. A Newtonian Perturbation Approximation

A certain degree of simplification is possible in the foregoing perturbation problem if the limit

$$\epsilon/\lambda \downarrow 0 \tag{40a}$$

$$\lambda \equiv (\gamma-1)/(\gamma+1) \tag{40b}$$

is applied over and above (3). Because of this simplification, the previous considerations can now be generalized to bodies of the form given by (11). If regions that scale as the Mach angle and are inside the shock layer are considered, then for

Table 2 Cross flow velocities at boundaries

θ Range	R_B	v_B	w_B
$0 < \theta < \theta_0$	1	1	0
$\theta_0 < \theta < \pi - \theta_0$	$(1/B)\csc\theta$	$\frac{1}{2}p_S\,\text{ctn}\theta$	$-[\gamma(\gamma-1)/2]^{1/2}G'(\text{ctn}\theta)$
$\pi - \theta_0 < \theta < \pi$	1	-1	0

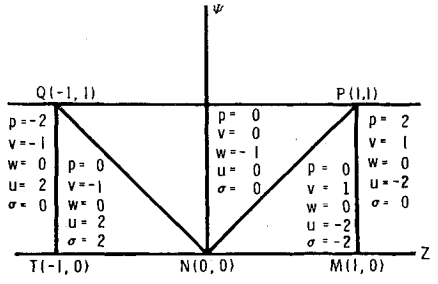

Fig. 6 Differential flap solution.

(41) the flow properties have the following asymptotic representations:

$$p(x,\psi,z;\ \gamma) = p^*(x^*,\psi^*,z^*) + \ldots \quad (41a)$$

$$v(x,\psi,z;\ \gamma) = v^*(x^*,\psi,z^*) + \ldots \quad (41b)$$

$$w(x,\psi,z;\ \gamma) = \lambda^{-1/2}w^*(x^*,\psi^*,z^*) + \ldots \quad (41c)$$

$$g(x,z;\ \gamma) = g^*(x^*,z^*) + \ldots \quad (41d)$$

$$f(x,z) = f^*(x^*,z^*) \quad (41e)$$

where

$$x^* = x,\ \psi^* = \lambda^{-1}\psi,\ z^* = \lambda^{-1/2}z \quad (42)$$

Substitution of (41) and (42) into (13) and (14) gives the following problem for the starred quantities:

$$v^*_{\psi^*} + w^*_{z^*} = 0 \quad (43a)$$

$$p^*_{\psi^*} + v^*_{z^*} = 0 \quad (43b)$$

$$w^*_{z^*} = 0 \quad (43c)$$

$$v_B \equiv v(x,0,z) = v^*(x^*,0,z^*) = f^*_{z^*} \quad (44a)$$

$$p^*_S \equiv p^*(x^*,x^*,z^*) = 2v^*_S = 2g^*_{x^*} \quad (44b)$$

$$w^*_S = -g^*_{z^*} \quad (44c)$$

The solution of the foregoing equations discussed in Ref. 6 will not be given here since the procedure is relatively straightforward. By this procedure it is found that

$$v = f_x(x,z) - g_\psi(\psi,z) - f_\psi(\psi,\tilde{z}) \quad (45a)$$

$$w = -g_z(\psi,z) \quad (45b)$$

$$p = 2g_x(x,z) + (x - \psi)f_{xx}(x,z) \quad (45c)$$

$$2g = \int_{z-x}^{z} f_x(x - z + \tilde{z},\tilde{z})d\tilde{z} + \int_{z}^{z+x} f_x(x + z - \tilde{z},\tilde{z})d\tilde{z} \quad (45d)$$

where the star notation has been dropped. In particular, the pressure on the body surface is given by

$$p_B = p(x,0,z) = xf_{xx}(x,z) + \int_{z-x}^{z} \frac{\partial}{\partial(x - z + \tilde{z})} f_x(x - z + \tilde{z},\tilde{z})d\tilde{z} + \int_{z}^{z+x} \frac{\partial}{\partial(x + z - \tilde{z})} f_x(x + z - \tilde{z},\tilde{z})d\tilde{z} \quad (46)$$

Upon specialization of Eqs. (45) and (46) to the differential flap configuration considered in the previous sections, that is, if

$$f = x\ \mathrm{sgn}z \quad (46a)$$

$$g = xG(Z) \quad (46b)$$

and

$$\Psi \equiv \psi/x \qquad Z \equiv z/x \quad (47)$$

the following solution is obtained:

$$2G = (Z + 1)\ \mathrm{sgn}(Z + 1) - (Z - 1)\ \mathrm{sgn}(Z - 1) \quad (48a)$$

$$p = \mathrm{sgn}(Z + 1) + \mathrm{sgn}(Z - 1) \quad (48b)$$

$$-u = 2v = \mathrm{sgn}(Z + \Psi) + \mathrm{sgn}(Z - \Psi) \quad (48c)$$

$$2w = \mathrm{sgn}(Z - \Psi) - \mathrm{sgn}(Z + \Psi) \quad (48d)$$

$$\sigma = p - 2v = \mathrm{sgn}(Z + 1) + \mathrm{sgn}(Z - 1) - \mathrm{sgn}(Z + \Psi) - \mathrm{sgn}(Z - \Psi) \quad (48e)$$

Figure 6 shows a schematic representation of the flow field. Here, the line PQ is the trace of the shock surface, the lines PM and QT are the traces of the degenerate Mach cone, and NP and NQ are slip surfaces. The implication with respect to these traces is that they may be imagined as the projection of the pertinent boundaries in the plane $x = 1$. The flow quantities take on the indicated values in the regions shown in the figure according to the foregoing formulas.

As has been suggested previously, the shock shape in the degenerate three-dimensional region $\Psi^2,Z^2 < 1$ is

$$G = Z \quad (49)$$

It is evident that a sidewash discontinuity exists at the points of attachment to the outlying section Q and P, for which $G = \mathrm{sgn}Z$.

The trend to the shape given by Eq. (49) is already apparent in Fig. 4c for $\gamma = 1.4$. However, in contrast to the case for which $\gamma \neq 1$, the Newtonian flow field contains slip surfaces trailing from the shock wave. These vortex sheets result from the discontinuity in the shock slopes g_x at points P and Q.

The Mach surfaces PM and QT (Fig. 6) play the role of secondary waves that arise as a result of the primary interaction of the central shock and its outlying sections. These secondary waves are required to make the slip surfaces NP and NQ identical with stream surfaces. The high background density and momentum of the basic wedge flow as $\gamma \to 1$ impedes this mechanism, resulting in pressure jumps across the Mach waves without corresponding velocity discontinuities to this order. As a result, the particle paths appear to pass through the slip surfaces exhibiting kinks unsupported by corresponding pressure jumps. From another viewpoint, the slip surfaces of the first-order flow are stream surfaces of the zeroth-order basic wedge flow and, as such, do not contain the first-order streamlines.

Despite the plausibility of the foregoing arguments and the fact that the solution (48) is entirely consistent within the accuracy of the approximations employed, with the momentum conservation laws across discontinuity surfaces, the singular nature of the flow field raises some doubts about the validity of the specialization of the general formulas (45) to the special shape (46a). In particular, the effect of these singularities is to produce nonuniformities in the representations of the dependent variables about the undisturbed boundaries. These representations, it is recalled, were used in the formulation of the boundary conditions. To what approximation, if any, (48) is a solution to the more accurate functional equations that result when the boundary linearizations are discarded, is a matter for future research.

VI. Conclusions

Various perturbations on hypersonic wedge flow have been analyzed within the framework of hypersonic small disturbance theory. In particular, the conical field over a differential flap configuration has been determined. More general distortions are treated under the assumption that γ, the specific heat ratio, is near unity. The surface pressure distributions obtained in this analysis for a hypersonic wing with the differential flap configuration indicate that, generally, the rolling

moment is reduced by the three-dimensional interactions from what it would be if the field were purely two-dimensional.

Further work has been initiated to extend the considerations to perturbations on cones. Because of the increase in complexity of the HSDT equations, it would seem that the Newtonian approximation should be applied at the outset for this case.

References

[1] Van Dyke, M. D., "A study of hypersonic small disturbance theory," NACA Rept. 1194 (1954).

[2] Hayes, W. and Probstein, R., *Hypersonic Flow Theory* (Academic Press, New York, 1959), Chap. II.

[3] Cole, J. D., "Newtonian flow theory for slender bodies," J. Aeronaut. Sci. **24**, 448–455 (1957).

[4] Guiraud, J. P., "Ecoulements hypersoniques infiniment voisins de l'ecoulement sur un diedre," Compt. Rend. **224**, 2281–2284 (1957).

[5] Holt, M. and Yim, B., "Supersonic flow past finite double wedge wings of variable thickness," Parts I and II, Air Force Office of Scientific Research TN 60-431, 2 (1960).

[6] Malmuth, N., "Perturbations on hypersonic wedge flow," Ph. D. Thesis, California Institute of Technology (1962).

[7] Busemann, A., "Infinitesimal conical supersonic flow," NACA TM 1100 (1947).

[8] Lagerstrom, P., "Linearized theory of conical wings," NACA TN 1685 (1948).

AUGUST 1964 AIAA JOURNAL VOL. 2, NO. 8

Laminar, Transitional, and Turbulent Heat Transfer after a Sharp Convex Corner

VICTOR ZAKKAY,* KAORU TOBA,† AND TA-JIN KUO‡

Polytechnic Institute of Brooklyn, Freeport, N. Y.

A flow model has been previously developed for treating the boundary-layer characteristics downstream of a surface discontinuity. The flow field in the neighborhood of the discontinuity or a sharp corner is divided into three regions: the flow upstream of the discontinuity which is obtained by standard techniques, that immediately downstream which is obtained by expanding both the supersonic and subsonic flow fields upstream of the discontinuity inviscidly around the corner, and that downstream of the discontinuity. The flow in the last region is represented by a viscous nonsimilar sublayer that starts at the discontinuity and by a viscous shear layer that has the profiles immediately downstream of the discontinuity as initial conditions. Based upon this flow model, analysis has been developed using the inner and outer expansion techniques. It is the purpose of this report to improve on the treatment of the laminar analysis and to extend the technique of application of this model to include turbulent and transitional flow downstream of the corner. Finally, the results are compared with some of the experimental data available in the literature. It is indicated that good agreement was obtained.

Nomenclature

c = const = $\rho\mu$
C_1 = constant defined in Eq. (3a)
D = constant defined in Eq. (9)
$f_0(\eta)$, $f_{1/2}(\eta)$, $f_{1/2\ 1/2}(\eta)$, $f_1(\eta)$ = functions of η (see Ref. 2)
$g_0(\eta)$, $g_1(\eta)$ = functions of η (see Ref. 2)
h = enthalpy
H = total enthalpy
M = Mach number
Nu = Nusselt number
p = pressure
Pr = Prandtl number
q = amount of heat transferred at the wall per unit time and unit area
Re_s = Reynolds number defined by $\rho_{se}(H_{ei})^{1/2}R_0/\mu_{se}$
R_0 = reference length
s = $\int_0^x \rho_{ei}\mu_{ei}u_e dx$
u, U = velocity components x direction
v = velocity component in y direction
x, y = Cartesian coordinates
δ = thickness of shear layer (or boundary layer)
θ = momentum thickness
κ = coefficient of heat conduction
μ = coefficient of viscosity
ν = coefficient of kinematic viscosity
ρ = density
σ = measure of vorticity gradient defined in Eq. (3)
τ = variable defined in Eq. (3)
Φ = measure of curvature of enthalpy profile defined in Eq. (3)
ψ = stream function
ω = measure of vorticity defined in Eq. (3)
Ω = measure of slope ine nthalpy profile definedin Eq. (3)

Subscripts

ei = condition external to shear layer
se = stagnation condition after normal shock
$*$ = reference state

Received July 17, 1963; revision received January 28, 1964. The study was supported by the Air Force Office of Scientific Research Grant No. AF-AFOSR-1-63.

* Research Associate Professor, Aerospace Engineering; now at New York University, New York. Member AIAA.

† Research Associate; now at Douglas Aircraft Company, Los Angeles, Calif. Member AIAA.

‡ Graduate Assistant; now at Pennsylvania State University, University Park, Pa.

Introduction

IN many practical problems in hypersonic flight, bodies having surface discontinuities or regions with rapid variation of curvature are used. Typical bodies of such type are, for example, cone-cylinder combinations.

A sublayer model for the boundary-layer characteristics downstream of the corner was first introduced by Sternberg.[1]